Oscillating carbon nanotori along carbon nanotubes

Tamsyn A. Hilder* and James M. Hill†

Nanomechanics Group, School of Mathematics and Applied Statistics, University of Wollongong, New South Wales 2522, Australia

(Received 2 August 2006; revised manuscript received 18 December 2006; published 13 March 2007)

The discovery of carbon nanostructures, such as nanotubes and C_{60} fullerenes, has given rise to a number of potential nanoscale devices. One such device is the gigahertz oscillator, comprising an inner shell sliding inside an outer shell of a multiwalled carbon nanotube, and which, at least theoretically, generates oscillatory frequencies in the gigahertz range. Following the concept of these gigahertz oscillators and the recent discovery of "fullerene crop circles," here we propose the notion of a nanotorus-nanotube oscillator comprising a carbon nanotorus which is sucked by the van der Waals force onto the carbon nanotube, and subsequently oscillates along the nanotube axis due to the equal and opposite pulselike forces acting at either end of the nanotube. Assuming a continuum approach, where the interatomic interactions are replaced by uniform atomic surface densities, and assuming that the geometry of the nanotube and nanotorus is such that the nanotorus always remains symmetrically situated around the nanotube, we present the basic mechanics of such a system, including the determination of the suction and acceptance energies, and the frequency of the resulting oscillatory motion. In contrast to the previously studied gigahertz nanoscale oscillators, here the oscillatory frequencies are shown to be in the megahertz range. Our study, although purely theoretical must necessarily precede any experimental implementation of such oscillatory systems.

DOI: 10.1103/PhysRevB.75.125415 PACS number(s): 81.07.De, 85.35.Kt

I. INTRODUCTION

The discovery[1] in 1991 that carbon nanotubes could be grown without a catalyst generated considerable research into numerous potential applications ranging from prospective applications in biology to electronics. Carbon nanotubes may be envisaged as one or many graphene sheets rolled up into a seamless hollow cylinder to form either single-wall or multiple-wall carbon nanotubes, respectively. They have many fascinating and unique mechanical and electronic properties, including but not limited to, their high strength and flexibility, low density, completely reversible deformation, and their ability to be either metallic or semiconducting depending on their physical structure. One potential device is demonstrated by the application of carbon nanotubes as high-frequency nanoscale oscillators, which are able to overcome the difficulties faced by micromechanical oscillators in attaining frequencies in the gigahertz range. Potential practical applications of such a device might include ultrafast optical filters for fiber optic systems and nanoantennae sensitive to high-frequency electromagnetic signals.

The unique properties of carbon nanotubes have led to many investigations into their mechanical properties. Yu *et al.*[2] investigated the strength and breaking mechanisms of multi-walled carbon nanotubes under tensile load. Their experiments indicate that the low shear strength between layers is due to the relatively weak van der Waals interactions between layers. Cumings and Zettl[3] subsequently investigated this result by controlled and reversible extrusion of the inner shell. Their experiments show that the inner-shell resistance force against sliding of the core is negligibly small, realizing ultralow friction.

The ultralow friction observed by Cumings and Zettl[3] was further investigated by Guo *et al.*,[4] Servantie and Gaspard,[5] and Rivera *et al.*[6] The interlayer resistance force against sliding, although small when compared to the van der Waals force, can prevent sustained oscillation as a result of the friction induced energy dissipation.[4] Servantie and Gaspard[5] also concluded that friction is small relative to the van der Waals force, by two orders of magnitude. Similarly, Rivera *et al.*[6] found that the frictional force is several orders of magnitude smaller than the van der Waals force.

The result of Cumings and Zettl[3] led Zheng and Jiang[7] to propose the concept of a nano-oscillator in which the inner shell oscillates inside the outer shell of a multiwalled carbon nanotube, which may be shown theoretically to operate at frequencies of up to several gigahertz. Zheng and Jiang[7] also show that decreasing the length of the inner tube further increases the oscillation frequency, giving rise to the possibility that a C_{60} fullerene, or buckyball, might provide the ultimate oscillating core in terms of realizing the highest oscillation frequency. Further studies, including mathematical models and molecular dynamics simulations, also predict frequencies in the gigahertz range. Legoas *et al.*[8] observed frequencies as high as 38 GHz through molecular dynamics simulations. Liu *et al.*[9] studied the oscillation of a C_{60} fullerene inside a carbon nanotube using molecular dynamics simulations and confirmed the prediction of Zheng and Jiang[7] by observing a frequency as high as 74 GHz.

Earlier studies find a minimum radius[10] (6.27 Å) of nanotube that can accept a C_{60} fullerene, and other studies[11,12] of the C_{60}-nanotube oscillator find that the C_{60} fullerene is sucked into one end of the nanotube, as a result of the highly attractive interatomic van der Waals potential. Such suction behavior does not always occur, and precise notions and definitions of suction and acceptance energies were formulated by Cox *et al.*,[13] and an acceptance condition was given prescribing whether or not a buckyball will be sucked into the nanotube by the van der Waals force alone. Cox *et al.*[14] also used mathematical modeling techniques to determine the oscillation frequency of the C_{60}-nanotube oscillator and obtained comparable results to those obtained through molecular dynamics simulations.

Liu *et al.*[15] observed single continuous toroidal carbon nanotubes in experiments, and subsequently introduced the term "fullerene crop circles." Seamless toroidal single-walled carbon nanotubes, with a tube diameter of 10 to 12 Å and a ring diameter of 3000 to 5000 Å are regularly observed. During formation the tube ends align themselves so as to maximize the van der Waals interactions, and then join together seamlessly through covalent bonding to form a perfect torus. Sano *et al.*[16] found that once formed the rings are quite stable both chemically and physically. It has been shown to be possible to form these toroidal nanotubes from straight single-walled carbon nanotubes,[17] where the ring circumference is therefore equal to the initial tube length. Using molecular dynamics simulations Huhtala *et al.*[18] and Han[19] investigated the stability of these toroidal carbon nanotubes and found much smaller ring diameters are possible than those discovered experimentally. For example, Huhtala *et al.*[18] found that a ring diameter of 220 Å must have a tube diameter below 13 Å for the nanotorus to remain stable and similarly Han[19] found ring diameters must be greater than 100, 200, and 400 Å for a nanotorus (5,5), (8,8), and (10,10), respectively to remain energetically stable. Effectively the toroidal nanotube structure can be viewed as a single-walled carbon nanotube closed around onto itself into a perfect torus. In this paper these toroidal structures are referred to as nanotori.

In view of the fact that at the nanoscale there may be many examples of oscillating systems and following the concept of gigahertz oscillators, here we propose the notion of a nanotorus-nanotube oscillator, comprising a nanotorus which is sucked onto a single-walled carbon nanotube and subsequently oscillates along its length. Previous research into gigahertz oscillators has been predominantly through molecular dynamics simulations. Here we use elementary mechanical principles and classical applied mathematical modeling techniques to formulate ideal model behavior, following that formulated by Cox *et al.*[13,14] for the C_{60}-nanotube oscillator. The aim of this work is to investigate the interaction of the nanotorus and the nanotube, to determine the resulting energy of the system, acceptance, and suction energies, and finally to analyze the oscillatory behavior. As far as the authors are aware such a device has yet to be constructed and the aim here is to assess its feasibility by consideration of the basic mechanics. Although these potential nanoscale devices are speculative in nature such a study must inevitably precede any practical implementation.

Following Cumings and Zettl,[3] and as a first attempt to model this system, we ignore frictional effects. In any real physical system inevitably frictional forces will occur, however, as detailed above, the existing evidence[3–6] suggests that frictional forces are much less than the van der Waals interaction force, sometimes by several orders of magnitude.[6] In addition, in order to further simplify the problem, we choose the geometric parameters of the nanotube and nanotorus such that the nanotorus always remains symmetrically located around the nanotube, by ensuring that the stability condition is satisfied so that the minimum energy position of the nanotorus occurs on the nanotube axis. It is shown that there are equal and opposite pulselike forces acting at both ends of the nanotube which we approximate by δ functions, and these large forces subsequently cause the nanotorus to oscillate along the nanotube and also prevent the nanotorus from sliding off the ends of the nanotube (note we assume that isothermal conditions prevail and therefore ignore thermal dissipation effects). While it is shown that all nanotori will be accepted onto the exterior of a carbon nanotube, there are clearly geometric constraints that the nanotorus ring radius must exceed the sum of the nanotube radius plus the nanotorus tube radius. The closer the nanotube radius and nanotorus ring radius are in magnitude the greater the oscillation frequency. In contrast to previously studied nanoscale gigahertz oscillators,[13,14] the resulting oscillatory frequencies determined here are in the megahertz range. A possible advantage of the present system may be the ease of manufacture, as the nanotorus and nanotube may be more easily manipulated with techniques such as optical tweezers.

In the following section we outline the Lennard-Jones potential, which is widely used as the interatomic potential in the modeling of nonbonded interactions. Following this the stability condition is established which ensures that the nanotorus remains symmetrically located about the nanotube axis, and the geometric parameters adopted are shown to satisfy this condition. We then determine the Lennard-Jones energy of the nanotorus-nanotube interaction, followed by an evaluation of the van der Waals interaction force, acceptance, and suction energies, and finally the predicted oscillatory frequencies. Three appendixes are included which contain various analytical details.

II. EVALUATION OF ENERGY

A. Lennard-Jones potential

The nonbonded interaction energy is defined by

$$E = \eta^2 \int \int \nu(\rho) d\Sigma_1 d\Sigma_2, \tag{1}$$

where $\nu(\rho)$ is the potential function for two molecules a distance ρ apart and $d\Sigma_1$ and $d\Sigma_2$ are surface elements on the nanotorus and nanotube, respectively. Following conventional practice, the atoms are assumed to be uniformly distributed over the surface of the molecule in a continuum approximation, where η represents the mean surface density of the carbon atoms. We assume both the nanotorus and nanotube have the same surface density, approximated as the mean surface density of graphene[9] 0.382 atoms/Å^2. The inverse power model, the so-called Lennard-Jones potential, is used in this investigation and is given by

$$\nu(\rho) = -A\rho^{-6} + B\rho^{-12}, \tag{2}$$

where A and B are the attractive and repulsive constants, respectively, and here we use $A=15.2$ eV Å (Ref. 6) and $B=24.1\times10^3$ eV Å (Ref. 12) for the interaction between graphene-graphene.[10]

B. Stability condition

Before we evaluate the interaction energy it is important to adopt those geometric parameters which ensure stability

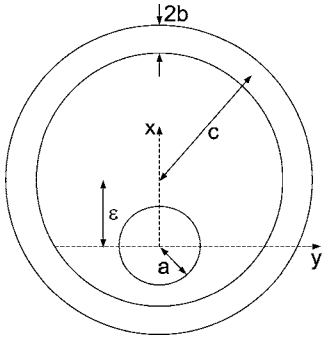

FIG. 1. Cross section of nanotorus offset a distance ϵ from nanotube axis.

where the nanotorus is symmetrically located about the nanotube axis. For this position to be stable the first derivative must vanish and the second derivative of the energy must be positive.

We suppose that the nanotorus is offset a distance ϵ from the z axis of the nanotube, as shown in Fig. 1. A typical point on the nanotube is defined by

$$x_1 = a\cos\Theta, \quad y_1 = a\sin\Theta, \quad z_1 = z,$$

and on the nanotorus

$$x_2 = (c + b\cos\phi)\cos\theta + \epsilon, \quad y_2 = (c + b\cos\phi)\sin\theta,$$

$$z_2 = b\sin\phi.$$

The distance between a typical point on the surface of the nanotorus and a typical point on the surface of the nanotube is given by

$$\begin{aligned}\rho^2 &= (x_1 - x_2)^2 + (y_1 - y_2)^2 + (z_1 - z_2)^2 \\ &= [(c + b\cos\phi) - a]^2 \\ &\quad + \epsilon^2 + 2\epsilon[(c + b\cos\phi)\cos\theta - a\cos\Theta] \\ &\quad + 4a(c + b\cos\phi)\sin^2[(\Theta - \theta)/2] + (b\sin\phi - z)^2.\end{aligned} \tag{3}$$

Substituting Eq. (2) into Eq. (1), the resulting interaction energy is thus

$$E = ab\eta^2 \int_{-\infty}^{\infty}\int_0^{2\pi}\int_0^{2\pi}\int_0^{2\pi}\left(\frac{-A}{\rho^6} + \frac{B}{\rho^{12}}\right) \times (c + b\cos\phi)d\theta d\phi d\Theta dz,$$

where ρ is given by Eq. (3) and we consider an infinite nanotube. After the z integration we obtain

$$E = \frac{3\pi ab\eta^2}{8}\int_0^{2\pi}\int_0^{2\pi}\int_0^{2\pi}\left(-\frac{A}{\alpha_1^{5/2}} + \frac{21B}{32\alpha_1^{11/2}}\right) \times (c + b\cos\phi)d\theta d\phi d\Theta, \tag{4}$$

where

TABLE I. Geometric parameters providing stability.

a (Å)	b (Å)	c (Å)
8.14	3.92	15.6
10.856	3.39	15
16.95	3.39	24
16.95	6.78	27.4
25.77	4.07	33
25.77	6.78	36
47.75	3.39	55
48.21	3.39	55

$$\begin{aligned}\alpha_1 &= (c + b\cos\phi - a)^2 + \epsilon^2 + 2\epsilon(c + b\cos\phi)\cos\theta \\ &\quad - 2a\epsilon\cos\Theta + 4a(c + b\cos\phi)\sin^2[(\Theta - \theta)/2].\end{aligned}$$

Further details of the derivation of Eq. (4) are given in Appendix A. We are only interested in the stability of the system at $\epsilon=0$, in other words we wish to ensure a minimum energy position, thus

$$\left.\frac{\partial E}{\partial \epsilon}\right|_{\epsilon=0} = 0, \quad \left.\frac{\partial^2 E}{\partial \epsilon^2}\right|_{\epsilon=0} > 0, \tag{5}$$

which for particular values of the geometric parameters a, b, and c we may confirm numerically.

We may now select those geometric parameters for which Eq. (5) is satisfied and Table I gives some typical values of such parameters. In general, the closer the nanotube and nanotorus ring radii, the more likely a stable configuration occurs at $\epsilon=0$. In the following subsections all geometric parameters considered are such that Eq. (5) is satisfied.

C. Nanotorus-nanotube interaction energy

In this section we determine the interaction energy between the nanotube and nanotorus. We suppose that the distance between the center of the nanotorus ring and the axial center of the nanotube is defined by Z, as indicated in Fig. 2. Similarly, a typical point on the nanotube is defined by

$$x_1 = a\cos\Theta, \quad y_1 = a\sin\Theta, \quad z_1 = z,$$

and on the nanotorus

$$x_2 = (c + b\cos\phi)\cos\theta, \quad y_2 = (c + b\cos\phi)\sin\theta,$$

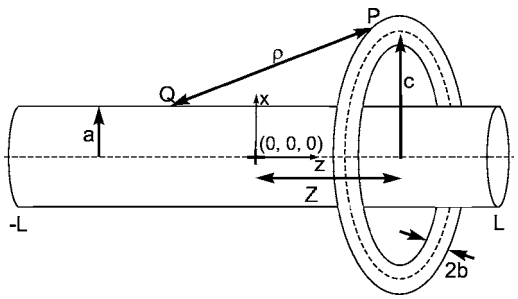

FIG. 2. Nanotorus oscillating along the exterior of a nanotube.

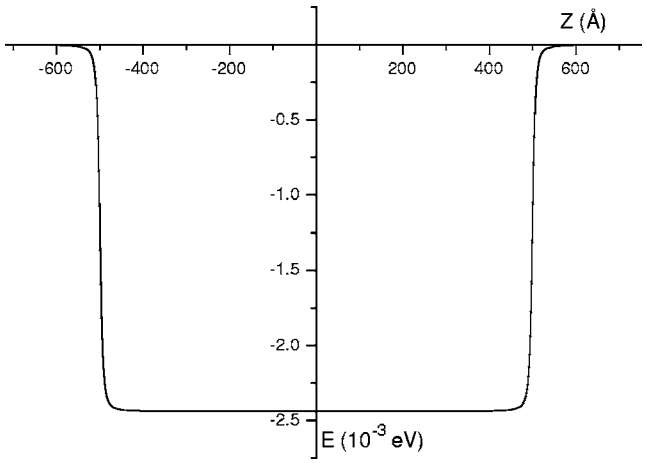

FIG. 3. Lennard-Jones potential energy E against nanotorus position Z.

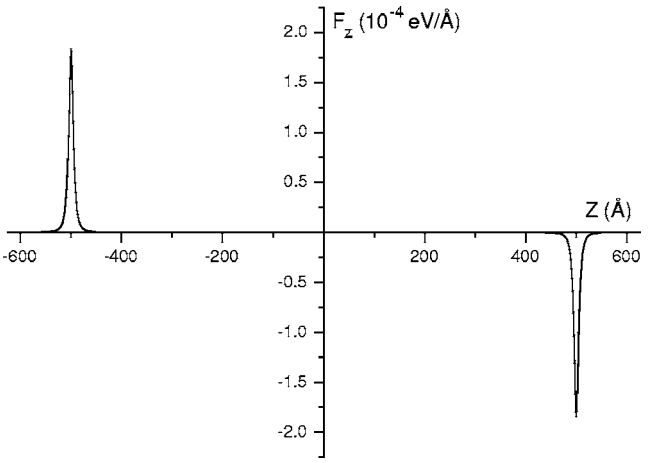

FIG. 4. Axial force against nanotorus position Z.

$$z_2 = Z + b \sin \phi.$$

The distance between a typical point on the surface of the nanotorus and a typical point on the surface of the nanotube is given by

$$\begin{aligned}\rho^2 &= (x_1 - x_2)^2 + (y_1 - y_2)^2 + (z_1 - z_2)^2 \\ &= [(c + b\cos\phi) - a]^2 \\ &\quad + [(z - Z) - b\sin\phi]^2 + 4a(c + b\cos\phi)\sin^2[(\Theta - \theta)/2].\end{aligned} \tag{6}$$

Similarly, the resulting Lennard-Jones potential energy becomes

$$\begin{aligned}E = ab\eta^2 \int_{-L}^{L}\int_0^{2\pi}\int_0^{2\pi}\int_0^{2\pi}\left(\frac{-A}{\rho^6} + \frac{B}{\rho^{12}}\right) \\ \times (c + b\cos\phi)d\theta d\phi d\Theta dz,\end{aligned} \tag{7}$$

where ρ is given by Eq. (6), the length of the nanotube is $2L$, and we chose geometric parameters of the nanotube and nanotorus such that the stability condition given by Eq. (5) is valid. Details for evaluating Eq. (7) in terms of hypergeometric and Legendre functions are presented in Appendixes B and C. On making the approximation that $z \gg a, b, c$ the resulting Lennard-Jones potential energy is shown to be given by

$$\begin{aligned}E = 4\pi^3\eta^2 b\int_0^{2\pi}\left[\frac{-3A}{32(\beta+a)^2}P_{-1/2}^{-2}\left(\frac{(\beta+a)^2+4a\beta}{(\beta-a)^2}\right)\right. \\ \left. + \frac{945B(a\beta)^{-3/2}}{2048(\beta+a)^5}P_{-1/2}^{-5}\left(\frac{(\beta+a)^2+4a\beta}{(\beta-a)^2}\right)\right]\frac{(\lambda+\delta)d\phi}{(\beta-a)},\end{aligned} \tag{8}$$

where $\beta = c + b\cos\phi$, $P_\nu^\mu(z)$ is an associated Legendre function of the first kind, and

$$\lambda = \frac{L - Z - b\sin\phi}{[(\beta-a)^2 + (L - Z - b\sin\phi)^2]^{1/2}},$$

$$\delta = \frac{L + Z + b\sin\phi}{[(\beta-a)^2 + (L + Z + b\sin\phi)^2]^{1/2}},$$

and the remaining ϕ integration must be evaluated numerically.

Using the algebraic package MAPLE, in Fig. 3 we plot the Lennard-Jones potential energy given by Eq. (8) against the nanotorus position Z, where we use $c = 55$ Å, $b = 3.39$ Å from results of Han[19] and we choose a nanotube with radius $a = 48.21$ Å and half length $L = 500$ Å. These dimensions are such that Eq. (5) is satisfied and the nanotorus is always symmetrically located around the nanotube.

III. INTERACTION OF NANOTORUS WITH THE CARBON NANOTUBE

Due to the assumed symmetry of the problem we are only concerned with the force in the axial direction $F_z = -dE/dZ$, where E is given by Eq. (8). This is a reasonable assumption, provided the nanotorus remains symmetrically located around the nanotube, which is valid for those geometric parameters chosen to satisfy the stability condition given by Eq. (5). If this condition is not satisfied then the nanotorus might shift off axis and as a result forces normal to the z axis may exist, but this situation is far more complicated to analyze and it is not considered here. From Eq. (8) the interaction force between the carbon nanotorus and the carbon nanotube is given by

$$\begin{aligned}F_z = -4\pi^3\eta^2 b\int_0^{2\pi}\left[\frac{-3A}{32(\beta+a)^2}P_{-1/2}^{-2}\left(\frac{(\beta+a)^2+4a\beta}{(\beta-a)^2}\right)\right. \\ \left. + \frac{945B(a\beta)^{-3/2}}{2048(\beta+a)^5}P_{-1/2}^{-5}\left(\frac{(\beta+a)^2+4a\beta}{(\beta-a)^2}\right)\right](\beta-a) \\ \times(\bar{\delta}-\bar{\lambda})d\phi,\end{aligned}$$

where $\bar{\delta} = [(\beta-a)^2 + (L+Z+b\sin\phi)^2]^{-3/2}$ and $\bar{\lambda} = [(\beta-a)^2 + (L-Z-b\sin\phi)^2]^{-3/2}$. Figure 4 illustrates the interaction force F_z against the distance between the two centers Z, where again $c = 55$ Å, $b = 3.39$ Å, $a = 48.21$ Å, and $L = 500$ Å.

By integrating this force we obtain an expression for the work done by the van der Waals force. For the nanotorus to be accepted onto the nanotube from the leftmost end by the van der Waals force alone, the sum of its kinetic energy and the work done from $-\infty$ to Z_0, the point at which the force at the leftmost end becomes negative, must be positive. Following Cox *et al.*,[13] we therefore obtain the condition $E_{\mathrm{KE}}+E_a>0$, where E_{KE} is the kinetic energy and E_a is the work done from $-\infty$ to Z_0, termed the acceptance energy. If we assume that the nanotorus is initially at rest then the condition becomes $E_a>0$. In this case the force is always positive at the leftmost end and therefore the nanotorus is always accepted onto the nanotube, provided that the nanotorus ring radius is greater than the sum of the nanotube radius a plus the nanotorus tube radius b plus the interlayer distance of graphite (3.4 Å). We find that the closer the two objects are in radii, the greater the acceptance energy since the interaction energy is increased as a result of the close proximity of atoms.

The amount of energy imparted on the nanotorus when it is sucked onto the nanotube is termed the suction energy[13] E_s, calculated by integrating the van der Waals force from $-\infty$ to 0, or the strength of one pulse. This suction energy can be used to calculate the oscillation velocity of the nanotorus evaluated in the following section, and is given by

$$E_s = -8\pi^3\eta^2 b\int_0^{2\pi}\left[\frac{-3A}{32(\beta+a)^2}P_{-1/2}^{-2}\left(\frac{(\beta+a)^2+4a\beta}{(\beta-a)^2}\right)+\frac{945B(a\beta)^{-3/2}}{2048(\beta+a)^5}P_{-1/2}^{-5}\left(\frac{(\beta+a)^2+4a\beta}{(\beta-a)^2}\right)\right]\frac{d\phi}{(\beta-a)}.$$

IV. OSCILLATION

In this section we determine the frequency of oscillation of the nanotorus. This can be determined from Newton's second law, thus

$$m\frac{d^2Z}{dt^2} = F_{\mathrm{vdW}}(Z) - F_r(Z),$$

where $F_{\mathrm{vdW}}(Z)=-dE/dZ$ since we are only concerned with the axial force, and $F_r(Z)$ is the frictional force. It has been shown by a number of researchers[3–6] that frictional forces are small in comparison to the van der Waals force, and in some cases by several orders of magnitude.[6] As a first approximation to this potential device we therefore ignore the effects of friction so that $F_r(Z)=0$. Although there may exist corrugation effects, these are neglected here due to the resulting high oscillation frequency.[5] Following Cox *et al.*,[14] $F_{\mathrm{vdW}}(Z)$ may be approximated by two Dirac δ functions, since the force is zero everywhere except at the ends, where there exist equal and opposite pulselike forces. We now multiply the equation by dZ/dt and integrate to obtain

$$\frac{m}{2}\left(\frac{dZ}{dt}\right)^2 = W[H(Z+L)-H(Z-L)]+\frac{mv_0^2}{2},$$

where $H(x)$ is the usual Heaviside function, W is the work done or strength of one pulse (the suction energy E_s), v_0 is the initial velocity of the nanotorus, and m is the mass of the nanotorus. We can use this equation and $f=v/4L$ to obtain the estimated oscillation frequency, where $H(Z+L)-H(Z-L)=1$ when $-L\leq Z\leq L$ and zero elsewhere. If we assume that there is no initial velocity then for the nanotorus-nanotube oscillator of $c=55$ Å, $b=3.39$ Å, $a=48.21$ Å, and $L=500$ Å we obtain a frequency of 18.67 MHz.

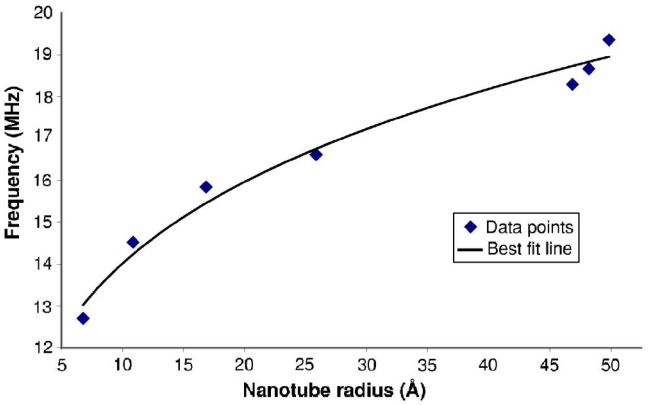

FIG. 5. (Color online) Frequency of oscillation for nanotorus ($b=3.39$ Å, $c=55$ Å) as a function of the nanotube radius a.

Figures 5 and 6 illustrate how the frequency varies with nanotube radius and nanotorus ring radius, respectively. Minimizing the nanotorus ring radius has a greater effect on increasing the frequency of oscillation, since it also reduces the mass requiring movement along the nanotube. Figure 6 illustrates how reducing the ring radius increases the frequency. Potentially, the nanotorus-nanotube oscillator could reach frequencies as high as 0.13 GHz if the radii of the nanotorus and nanotube were as close as possible. The frequency of oscillation for this system is considerably less than the predicted gigahertz nanoscale oscillators[7–9,14] mentioned in Sec. I, however, a possible advantage of the nanotorus-nanotube oscillator may be ease of manufacture since a nanotube and nanotorus may be more easily manipulated with techniques such as optical tweezers.

V. CONCLUSIONS

We have examined the basic mechanics of a symmetrically situated nanotorus oscillating along the exterior of a

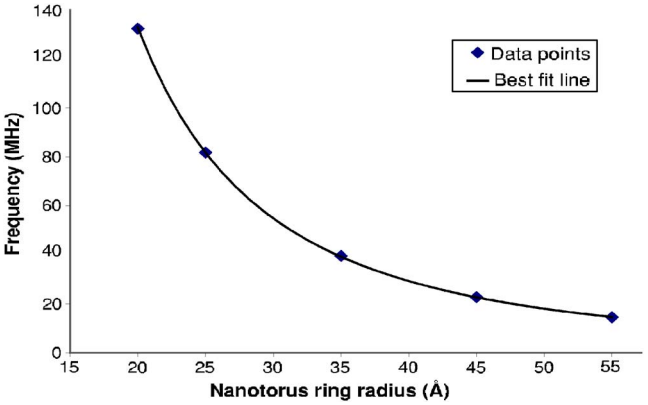

FIG. 6. (Color online) Frequency of oscillation for nanotorus ($b=3.39$ Å) oscillating along a nanotube ($a=48.21$ Å) as a function of the nanotorus ring radius c.

carbon nanotube, with a view to determining its feasibility as a nanoscale device. Following Cumings and Zettl,[3] and as a first attempt to model this system, we have ignored frictional effects. The geometric parameters of the nanotube and nanotorus are chosen to satisfy a stability condition which ensures that the nanotorus always remains symmetrically located around the nanotube. We show that there are equal and opposite pulselike forces operating at the nanotube extremities, which subsequently cause the nanotorus to oscillate along the nanotube and prevent the nanotorus from sliding off the ends of the nanotube. These pulselike forces can be approximated by Dirac δ functions to determine a predicted oscillatory frequency. In contrast to previously studied nanoscale oscillators, the resulting oscillatory frequencies are in the megahertz range. We believe this arises as a consequence of the lower suction energy and the significantly higher mass of a nanotorus in comparison to a C_{60} fullerene. A possible advantage of the present system may be the ease of manufacture in terms of manipulating the nanotube and nanotorus using techniques such as optical tweezers.

In principle, a nanotori with ring radii greater than the sum of the nanotube radius a plus the nanotorus tube radius b plus the interlayer distance of graphite (3.4 Å) will always be accepted onto the carbon nanotube. We find that the maximum acceptance energy occurs when the radii of the nanotorus and nanotube are as close as possible. Similarly, this will also provide the greatest frequency of oscillation and ensure stability where the nanotorus is symmetrically located around the nanotube axis.

ACKNOWLEDGMENT

We gratefully acknowledge the support from the Discovery Project Scheme of the Australian Research Council and the University of Wollongong.

APPENDIX A: EVALUATION OF z INTEGRATION FOR EQ. (4)

We simplify Eq. (3), thus

$$\rho^2 = \alpha_1 + (\alpha_2 - z)^2,$$

where $\alpha_1 = (c + b\cos\phi - a)^2 + \epsilon^2 + 2\epsilon(c + b\cos\phi)\cos\theta - 2a\epsilon\cos\Theta + 4a(c + b\cos\phi)\sin^2[(\Theta - \theta)/2]$ and $\alpha_2 = b\sin\phi$. The integration becomes

$$J_n = \int_{-\infty}^{\infty} \frac{dz}{[\alpha_1 + (\alpha_2 - z)^2]^n},$$

where we are interested in the values $n=3$ and $n=6$. On making the substitution $\xi = \alpha_2 - z$ and $\xi = \alpha_1^{1/2}\tan\gamma$ we obtain

$$J_n = \int_{-\infty}^{\infty} \frac{d\xi}{(\alpha_1 + \xi^2)^n} = \alpha_1^{1/2-n} \int_{-\pi/2}^{\pi/2} \cos^{2n-2}\gamma d\gamma.$$

From Gradshteyn and Ryzhik[20] (p. 149) we obtain the result

$$J_3 = \frac{3\pi}{8\alpha_1^{5/2}}, \quad J_6 = \frac{63\pi}{256\alpha_1^{11/2}},$$

and the resulting interaction potential is

$$E = \frac{3\pi ab\eta^2}{8} \int_0^{2\pi}\int_0^{2\pi}\int_0^{2\pi} \left(-\frac{A}{\alpha_1^{5/2}} + \frac{21B}{32\alpha_1^{11/2}} \right) \times (c + b\cos\phi) d\theta d\phi d\Theta.$$

APPENDIX B: EVALUATION OF Θ INTEGRATION FOR EQ. (8)

We simplify Eq. (6) to be

$$\rho^2 = C_1 + C_2 \sin^2[(\Theta - \theta)/2],$$

where $C_1 = [(c + b\cos\phi) - a]^2 + [(z - Z) - b\sin\phi]^2$ and $C_2 = 4a(c + b\cos\phi)$. The Θ integration

$$I_n = \int_0^{2\pi} \frac{d\Theta}{\{C_1 + C_2 \sin^2[(\Theta - \theta)/2]\}^{n/2}},$$

where we are interested in the two values $n=6$ and $n=12$. We now make the substitution $x = (\Theta - \theta)/2$ and note that the starting angle of integration is arbitrary so that

$$I_n = 2\int_{-\theta/2}^{\pi-\theta/2} \frac{dx}{[C_1 + C_2\sin^2 x]^{n/2}} = 2\int_0^{\pi} \frac{dx}{[C_1 + C_2\sin^2 x]^{n/2}} = 4\int_0^{\pi/2} \frac{dx}{[C_1 + C_2\sin^2 x]^{n/2}}.$$

On making the substitution $t = \cot x$ and letting $n = 2m$ we obtain the result

$$I_{2m} = 4\int_0^{\infty} \frac{(t^2+1)^{m-1}dt}{(C_1 t^2 + C_1 + C_2)^m} = \frac{4}{(C_1 + C_2)^m} \int_0^{\infty} \frac{(t^2+1)^{m-1}dt}{(C_3 t^2 + 1)^m},$$

where $C_3 = C_1/(C_1 + C_2)$. On making the further substitutions

$$z = t(1 + t^2)^{-1/2}, \quad t = z(1 - z^2)^{-1/2}, \quad dt = (1 - z^2)^{-3/2}dz, \tag{B1}$$

and $u = z^2$, we obtain the result in terms of hypergeometric functions

$$I_{2m} = \frac{2}{(C_1 + C_2)^m} \int_0^1 \frac{u^{-1/2}(1-u)^{-1/2}du}{[1 - (1 - C_3)u]^m} = \frac{2\pi}{(C_1 + C_2)^m} F\left(m, \frac{1}{2}; 1; \frac{C_2}{C_1 + C_2}\right). \tag{B2}$$

From Gradshteyn and Ryzhik[20] (p. 998) we have the transformation $F(\alpha, \beta; \gamma; -z) = (1+z)^{-\alpha} F[\alpha, \gamma - \beta; \gamma; z(1+z)^{-1}]$, where $\alpha = m$, $\beta = 1/2$, $\gamma = 1$, and $z = C_2/C_1$. We may deduce from Eq. (B2) that

$$I_{2m} = \frac{2\pi}{(C_1)^m} F\left(m, \frac{1}{2}; 1; \frac{-C_2}{C_1}\right),$$

where we are interested in the two values $m=3$ and $m=6$. From Erdélyi *et al.*[21] (p. 64) we note that we have a quadratic transformation, since two of the numbers $\pm(1-\gamma)$, $\pm(\alpha-\beta)$, $\pm(\alpha+\beta-\gamma)$ are equal and we note (p. 69) that it is also degenerate since at least one of the numbers α, β, $\gamma-\alpha$, γ

$-\beta$ is an integer. Using the transformation[21] $F(\alpha,\beta;\gamma;-z)=(1+z)^{\gamma-\alpha-\beta}F(\gamma-\alpha,\gamma-\beta;\gamma;-z)$ the hypergeometric function becomes

$$F(m,1/2;1;-z)=(1+z)^{1/2-m}F(1-m,1/2;1;-z)$$
$$=(1+z)^{1/2-m}\sum_{k=0}^{m-1}\frac{(1-m)_k(1/2)_k}{(1)_k}\frac{(-z)^k}{k!},$$

where $z=C_2/C_1$. The two cases $m=3$ and $m=6$ become simply

$$F(3,1/2;1;-z)=\frac{3z^2+8z+8}{8(1+z)^{5/2}},$$

$$F(6,1/2;1;-z)=\frac{63z^5+350z^4+800z^3+960z^2+640z+256}{256(1+z)^{11/2}}.$$

The resulting Lennard-Jones potential energy becomes

$$E=2\pi\eta^2ab\int_{-L}^{L}\int_0^{2\pi}\int_0^{2\pi}\left[\frac{-A}{(C_1)^3}F\left(3,\frac{1}{2};1;\frac{-C_2}{C_1}\right)\right.$$
$$\left.+\frac{B}{(C_1)^6}F\left(6,\frac{1}{2};1;\frac{-C_2}{C_1}\right)\right](c+b\cos\phi)d\theta d\phi dz, \tag{B3}$$

where $C_1=[(c+b\cos\phi)-a]^2+[(z-Z)-b\sin\phi]^2$ and $C_2=4a(c+b\cos\phi)$.

APPENDIX C: EVALUATION OF z INTEGRATION FOR EQ. (8)

By comparison of the relative size of z,a,b,c, assuming $z\gg a,b,c$, the dominant terms of Eq. (B3) simplify to give

$$E=2\pi\eta^2ab\int_0^{2\pi}\int_0^{2\pi}\int_{-L}^{L}\left[\frac{-A}{C_1^{1/2}(C_1+C_2)^{5/2}}\right.$$
$$\left.+\frac{B}{C_1^{1/2}(C_1+C_2)^{11/2}}\right](c+b\cos\phi)dzd\theta d\phi.$$

We can evaluate the z integral above for arbitrary n and substitute for C_1 and C_2

$$K_n=\int_{-L}^{L}\frac{dz}{[(\beta-a)^2+(z-Z-b\sin\phi)^2]^{1/2}[(\beta+a)^2+(z-Z-b\sin\phi)^2]^{n/2}},$$

where $\beta=c+b\cos\phi$ and we are interested in the values $n=5$ and $n=11$. On letting $z=Z+b\sin\phi+(\beta-a)\tan\omega$ we obtain

$$K_n=\int_{\omega_1}^{\omega_2}\frac{(\beta-a)\sec^2\omega d\omega}{[(\beta-a)^2(1+\tan^2\omega)]^{1/2}[(\beta+a)^2+(\beta-a)^2\tan^2\omega]^{n/2}}=\int_{\omega_1}^{\omega_2}\frac{\sec\omega d\omega}{[(\beta+a)^2+(\beta-a)^2\tan^2\omega]^{n/2}},$$

where

$$\omega_1=\tan^{-1}\left[\frac{-L-Z-b\sin\phi}{\beta-a}\right],$$

$$\omega_2=\tan^{-1}\left[\frac{L-Z-b\sin\phi}{\beta-a}\right].$$

We now make the substitution $t=\tan\omega$ so that we have

$$K_n=\int_{t_1}^{t_2}\frac{(t^2+1)^{-1/2}dt}{[(\beta-a)^2t^2+(\beta+a)^2]^{n/2}}$$
$$=\frac{1}{(\beta+a)^n}\left[\int_0^{t_2}\frac{(t^2+1)^{-1/2}dt}{(\gamma^2t^2+1)^{n/2}}+\int_{t_1}^{0}\frac{(t^2+1)^{-1/2}dt}{(\gamma^2t^2+1)^{n/2}}\right],$$

where $\gamma=(\beta-a)/(\beta+a)$, $t_1=\tan\omega_1$, and $t_2=\tan\omega_2$. For the second part of K_n we make a further substitution $t=-v$ to obtain

$$K_n=\frac{1}{(\beta+a)^n}\left[\int_0^{t_2}\frac{(t^2+1)^{-1/2}dt}{(\gamma^2t^2+1)^{n/2}}+\int_0^{-t_1}\frac{(t^2+1)^{-1/2}dt}{(\gamma^2t^2+1)^{n/2}}\right].$$

Again we make the substitution given by Eq. (B1) to get

$$K_n=\frac{1}{(\beta+a)^n}\left[\int_0^{\lambda}\frac{(1-z^2)^{n/2-1}dz}{[(\gamma^2-1)z^2+1]^{n/2}}\right.$$
$$\left.+\int_0^{\delta}\frac{(1-z^2)^{n/2-1}dz}{[(\gamma^2-1)z^2+1]^{n/2}}\right],$$

where the limits of integration are defined by

$$\lambda=\frac{L-Z-b\sin\phi}{[(\beta-a)^2+(L-Z-b\sin\phi)^2]^{1/2}},$$

$$\delta=\frac{L+Z+b\sin\phi}{[(\beta-a)^2+(L+Z+b\sin\phi)^2]^{1/2}}.$$

Making appropriate substitutions we obtain

$$K_n = \frac{1}{(\beta+a)^n}\left[\lambda\int_0^1 \frac{(1-\lambda^2 z^2)^{n/2-1}dz}{[1-(1-\gamma^2)\lambda^2 z^2]^{n/2}} + \delta\int_0^1 \frac{(1-\delta^2 z^2)^{n/2-1}dz}{[1-(1-\gamma^2)\delta^2 z^2]^{n/2}}\right].$$

On making the further substitution $u=z^2$, and from Bailey[22] (p. 77), we obtain two Appell's hypergeometric functions of two variables

$$K_n = \frac{1}{(\beta+a)^n}\left[\frac{\lambda}{2}\int_0^1 \frac{(1-\lambda^2 u)^{n/2-1}u^{-1/2}du}{[1-(1-\gamma^2)\lambda^2 u]^{n/2}} + \frac{\delta}{2}\int_0^1 \frac{(1-\delta^2 u)^{n/2-1}u^{-1/2}du}{[1-(1-\gamma^2)\delta^2 u]^{n/2}}\right]$$
$$= \frac{1}{(\beta+a)^n}\left[\lambda F\left(\frac{1}{2};\frac{n}{2},1-\frac{n}{2};\frac{3}{2};(1-\gamma^2)\lambda^2,\lambda^2\right) + \delta F\left(\frac{1}{2};\frac{n}{2},1-\frac{n}{2};\frac{3}{2};(1-\gamma^2)\delta^2,\delta^2\right)\right].$$

Again, comparing the relative size of terms $L \gg a,b,c,\beta$, we have $(1-\gamma^2)\lambda^2 \approx (1-\gamma^2)\delta^2 \approx 4a\beta/(\beta+a)^2$ and $\lambda^2 \approx \delta^2 \approx 1$, so that the above Appell's hypergeometric functions can be simplified using the identity given by Gradshteyn and Ryzhik[20] (p. 1010)

$$K_n = \frac{\sqrt{\pi}(\lambda+\delta)}{2(\beta+a)^n}\frac{\Gamma(n/2)}{\Gamma(1/2+n/2)}F\left(\frac{1}{2},\frac{n}{2};\frac{n+1}{2};\frac{4a\beta}{(\beta+a)^2}\right). \tag{C1}$$

From Erdélyi *et al.*[21] (p. 64) we again have a quadratic transformation, which is not degenerate but can be written as an associated Legendre function. Using the transformation from Gradshteyn and Ryzhik[20] (p. 960) we have

$$F\left(\frac{1}{2},\frac{n}{2};\frac{n+1}{2};x\right) = \Gamma\left(\frac{n+1}{2}\right)\frac{x^{(1-n)/4}}{(1-x)^{1/2}}P_{-1/2}^{(1-n)/2}\left(\frac{1+x}{1-x}\right),$$

where $x=4a\beta/(\beta+a)^2$ and $P_\nu^\mu(z)$ is an associated Legendre function of the first kind. Equation (C1) therefore becomes

$$K_n = \frac{\sqrt{\pi}(\lambda+\delta)}{2(\beta+a)^n}\Gamma\left(\frac{n}{2}\right)\frac{x^{(1-n)/4}}{(1-x)^{1/2}}P_{-1/2}^{(1-n)/2}\left(\frac{1+x}{1-x}\right)$$
$$= \frac{\sqrt{\pi}(\lambda+\delta)}{2(\beta-a)}\Gamma\left(\frac{n}{2}\right)\frac{(4a\beta)^{(1-n)/4}}{(\beta+a)^{(n-1)/2}}P_{-1/2}^{(1-n)/2}\left(\frac{(\beta+a)^2+4a\beta}{(\beta-a)^2}\right),$$

and we are interested in the two values $n=5$ and $n=11$. On noting that there is no longer any θ dependence, the resulting Lennard-Jones potential energy becomes

$$E = 4\pi^3\eta^2 b\int_0^{2\pi}\left[\frac{-3A}{32(\beta+a)^2}P_{-1/2}^{-2}\left(\frac{(\beta+a)^2+4a\beta}{(\beta-a)^2}\right) + \frac{945B(a\beta)^{-3/2}}{2048(\beta+a)^5}P_{-1/2}^{-5}\left(\frac{(\beta+a)^2+4a\beta}{(\beta-a)^2}\right)\right]\frac{(\lambda+\delta)d\phi}{(\beta-a)},$$

where $\beta=c+b\cos\phi$, $P_\nu^\mu(z)$ is an associated Legendre function of the first kind, and

$$\lambda = \frac{L-Z-b\sin\phi}{[(\beta-a)^2+(L-Z-b\sin\phi)^2]^{1/2}},$$

$$\delta = \frac{L+Z+b\sin\phi}{[(\beta-a)^2+(L+Z+b\sin\phi)^2]^{1/2}},$$

and the remaining ϕ integration must be evaluated numerically.

*Electronic address: tah429@uow.edu.au
†Electronic address: jhill@uow.edu.au

[1] S. Iijima, Nature (London) **354**, 56 (1991).
[2] M.-F. Yu, O. Lourie, M. J. Dyer, K. Moloni, T. F. Kelly, and R. S. Ruoff, Science **287**, 637 (2000).
[3] J. Cumings and A. Zettl, Science **289**, 602 (2000).
[4] W. Guo, Y. Guo, H. Gao, Q. Zheng, and W. Zhong, Phys. Rev. Lett. **91**, 125501 (2003).
[5] J. Servantie and P. Gaspard, Phys. Rev. B **73**, 125428 (2006).
[6] J. L. Rivera, C. McCabe, and P. T. Cummings, Nano Lett. **3**, 1001 (2003).
[7] Q. Zheng and Q. Jiang, Phys. Rev. Lett. **88**, 045503 (2002).
[8] S. B. Legoas, V. R. Coluci, S. F. Braga, P. Z. Coura, S. O. Dantas, and D. S. Galvão, Phys. Rev. Lett. **90**, 055504 (2003).
[9] P. Liu, Y. W. Zhang, and C. Lu, J. Appl. Phys. **97**, 094313 (2005).
[10] M. Hodak and L. A. Girifalco, Chem. Phys. Lett. **350**, 405 (2001).
[11] L. A. Girifalco, M. Hodak, and R. S. Lee, Phys. Rev. B **62**, 13104 (2000).
[12] D. Qian, W. K. Liu, and R. S. Ruoff, J. Phys. Chem. B **105**, 10753 (2001).
[13] B. J. Cox, N. Thamwattana, and J. M. Hill, Proc. R. Soc. London, Ser. A **463**, 461 (2006).
[14] B. J. Cox, N. Thamwattana, and J. M. Hill, Proc. R. Soc. London, Ser. A **463**, 477 (2006).
[15] J. Liu, H. Dai, J. H. Hafner, D. T. Colbert, R. E. Smalley, S. J. Tans, and C. Dekker, Nature (London) **385**, 780 (1997).
[16] M. Sano, A. Kamino, J. Okamura, and S. Shinkai, Science **293**, 1299 (2001).
[17] R. Martel, H. R. Shea, and P. Avouris, Nature (London) **398**, 299 (1999).
[18] M. Huhtala, A. Kuronen, and K. Kaski, Comput. Phys. Commun. **147**, 91 (2002).
[19] J. Han (unpublished).
[20] I. S. Gradshteyn and I. M. Ryzhik, *Table of Integrals Series and Products*, 6th ed. (Academic Press, New York, 1965).
[21] A. Erdélyi, W. Magnus, F. Oberhettinger, and F. G. Tricomi, *Higher Transcendental Functions* (McGraw-Hill, New York, 1953), Vol. 1, Chap. 2, pp. 56–119.
[22] W. N. Bailey, *Generalized Hypergeometric Series* (Hafner, New York, 1972).